THE JOURNAL OF PHYSICAL CHEMISTRY B

Article

A Microscopic Model of Singlet Fission

Paul Emery Teichen, and Joel David Eaves

J. Phys. Chem. B, **Just Accepted Manuscript** • DOI: 10.1021/jp208905k • Publication Date (Web): 15 May 2012

A Microscopic Model of Singlet Fission

Paul Teichen and Joel D. Eaves*

Department of Chemistry and Biochemistry, The University of Colorado at Boulder, Boulder, Colorado, 80309

E-mail: joel.eaves@colorado.edu

Abstract

Singlet fission, where an electronically excited singlet on one chromophore converts into a doubly excited state on two, has gone from a curiosity in organic photophysics to a potential pathway for increasing solar energy conversion efficiencies. Focusing on the role of solvent-induced energy level fluctuations that would be present in a dye-sensitized solar cell, we present a microscopic model for singlet fission that starts from an electronic model Hamiltonian. We construct diabatic states in a manifold of single and double excitations with total singlet multiplicity and then develop a multilevel nonMarkovian theory of dynamics for electronic populations in the presence of energy level fluctuations. Depending on the energy scales, energy gap fluctuations can either facilitate or hinder interconversion steps that lead to singlet fission. We critically assess the Markovian approximation that leads to golden rule rates and study the role of intramolecular solvation dynamics and electron transfer.

Keywords: dye-sensitized solar cells, thermal fluctuations, quantum master equation, electron transfer, multielectron dynamics

*To whom correspondence should be addressed

1 Introduction

Developing solar technology that is cost-competitive with fossil fuels will require considerable advances in fundamental science. In 1961, Schockley and Quiessler[1] argued that a single junction solar cell could never have power conversion efficiency larger than about 32 %. Their argument considered only the most basic physics; one photon absorbed above the band gap yields one electron hole pair, and that the cell is operating in steady-state. While these arguments are elementary, no single junction solar cell to date has broken the Shockley-Quiessler limit. To do so, a new generation of materials have been proposed that yield more than one electron hole pair per photon absorbed. In these materials, carriers that have energy in excess of the absorption threshold relax by emitting a second electron hole pair rather than cooling by phonon emission or other nonradiative relaxation pathways. Multiple exciton generation (MEG), the name given to this process in semiconductors and semiconducting nanocrystals, has received the most attention in recent years.[2–5] The great deal of debate surrounding the results and yields of MEG in nanocrystals highlights a fundamental weakness in our current understanding of the basic principles that might enable the one photon to multiple electron hole pair paradigm. Singlet fission is the molecular analog of MEG where a singlet excited state S_1 on one chromophore decays into two excitations T_1T_1 on different chromophores[6] (Figure 1). Unlike singlet to triplet conversion via intersystem crossing the initial and final states are simultaneous eigenstates of the total spin operator, $\mathcal{S}^2$, and the spin projection operator, $\mathcal{S}_z$. Singlet fission is a form of internal conversion from S_1 to T_1T_1, is spin-allowed, and may take place on the sub-picosecond timescale.[7–11]

Singlet fission was first invoked in the late 1960's to explain the photophysics of anthracene and tetracene crystals.[12,13] In the past 40 years, it has been observed in molecular crystals and quantified with a variety of methods.[6] But the potential of singlet fission in solar applications was not realized until 2006, when Hanna and Nozik[2] proposed that singlet fission chromophores could enhance the efficiency of dye-sensitized solar cells.[14,15] The singlet fission mechanism is highly system-specific. Singlet fission is a two-electron interconversion process that can proceed via direct coupling between the initial singlet excitation and the T_1T_1 states.[16,17] It may also occur

through concerted or stepwise electron transfer events that involve virtual or real intermediates, respectively.[6,18,19] Similar to the compounds studied in Refs. [18,20], we consider a class of chromophores whose relevant excited states can be described within frontier molecular orbital theory.[6] These states are weakly coupled, and the initial excited state is localized. Our treatment describes singlet fission within a stepwise, or "mediated" mechanism, in the language of Ref. [6]. Extensions of the model to higher-order perturbation theories that would describe concerted events through virtual state transitions, are straightforward.[21]

Clearly, computation has a role to play in locating molecules that might undergo singlet fission, but the calculations are demanding, and state of the art calculations are done with molecules in isolation. But dye-sensitized solar cells are in polar solutions[2–4,22] where interactions with solvent molecules induce electronic energy level fluctuations that can be on the order of 0.1-0.2 eV;[23–25] comparable to electronic energy level splittings of isolated singlet fission chromophores calculated with the highest available levels of theory.[16,26–30] Solvent polarization fluctuations enable transitions between states by activating the system and bringing it to a crossing point. They also dissipate energy of excited states[31] and stabilize products. From a design perspective, one may actually be able to exploit fluctuations to enable singlet fission when the energies of the S_1 and T_1T_1 states are not exactly degenerate. Clearly, a quantitative model of fluctuations needs to be part of a comprehensive theory for singlet fission.

In this manuscript, we develop a microscopic model of singlet fission that is capable of describing dynamics on picosecond and subpicosecond timescales in the presence of solvent induced energy level fluctuations. First, we propose a physically reasonable electronic model Hamiltonian based on frontier molecular orbital theory. We then derive an exact quantum master equation for the populations of the electronic states and analyze it in the limit of weak-coupling between electronic states. We analyze rate theories in the Markovian limit, when the timescale between relaxation is well-separated from the timescale for interconversion. Here, one imagines that solvation and relaxation timescales, as quantified through a time-dependent Stokes shift, are on the timescale of picoseconds, while interconversion timescales are at least an order of magnitude longer. The rate

theories align with the Förster/Dexter theory of energy and electron transfer.[32,33] Using plausible model parameters for the theory, we examine the nonMarkovian limit, where the system is prepared in such a way that the solvent is not in thermal equilibrium with the electrons. We then analyze the rate theory of a model that separates fluctuations from solvation dynamics and electron transfer kinetics. While phenomenological, the theory is microscopic. As a result, the inputs to the theory can come from a variety of sources: electronic structure calculations, molecular spectroscopy, and molecular dynamics.[34–37]

2 Methods

2.1 The electronic Hamiltonian

We begin by discussing a model electronic Hamiltonian. Recent work has suggested that the electronic levels in singlet fission systems can be modeled by considering the frontier molecular orbitals of two chromophores, termed left (L) and right (R). These chromophores could be different molecules, or different chromophores on the same molecule. Each chromophore has HOMO and LUMO energy levels separted by a gap, Δ. For the purposes of illustration, we consider identical chromophores. To construct a fairly general model, we clamp the nuclei at their equilibrium configurations and propose the following semiempirical electronic Hamiltonian,

$$H_{el} = H^0_{el} + W_{el} \,,$$

with

$$H^0_{el} = \sum_{k,\sigma} \epsilon_k n_{k,\sigma} + \mathcal{V} \sum_{\sigma,\sigma'} \left[n_{h_L,\sigma} n_{l_L,\sigma'} + n_{h_R,\sigma} n_{l_R,\sigma'} \right] + U \sum_{k,\sigma} n_{k,\sigma} n_{k,-\sigma} - X \sum_{\sigma} \left[n_{h_L,\sigma} n_{l_L,\sigma} + n_{h_R,\sigma} n_{l_R,\sigma} \right] , \tag{1}$$

and

$$W_{el} = - \sum_{j \neq k,\sigma} J_{jk} c^\dagger_{j,\sigma} c_{k,\sigma} \,. \tag{2}$$

The fermionic creation and destruction operators, $c^{\dagger}_{k,\sigma}$ and $c_{k,\sigma}$ respectively, create or destroy an electron in orbital k with spin σ. The ground state is a closed shell, and electrons can reside in the four frontier orbitals $\{h_L, l_L; h_R, l_R\}$ in either the spin up ($\sigma = \uparrow$) state or spin down ($\sigma = \downarrow$) state. The HOMO and LUMO basis functions are physically-motivated and mutually orthogonal, but do not necessarily represent the result of the real and virtual orbitals in an electronic structure calculation. ϵ_k is the "bare" energy of an electron in orbital k, U is the "Hubbard" on-site Coulomb integral of electrons in the same orbital, $\mathcal{V}$ the off-site Coulomb matrix element, and X is the exchange energy. Note that none of the terms in H^0_{el} couple different orbitals on different chromophores. The coupling matrix elements J_{jk} are two electron "resonance" integrals that do couple different orbitals between R and L chromophores. The resonance integrals represent the electron kinetic energy and allow electrons to move one at a time between orbitals by one-electron hops. The energy levels of H^0_{el} may be split by as much as 1 - 10 eV, while J has been calculated to be in the range of about 0.01 to 0.1 eV.[10,11,18] Solute-solvent energy scales, as quantified through the solvent-induced Stokes shift or electron transfer reorganization energies can be on the scale of 0.1 eV. These energy scales suggest that one can approach the singlet fission problem, at least for some of the chromophores for which these parameters are known, in the weak electronic coupling limit.

Figure 2 is an energy level diagram of some of the electronic configurations present in the representation of the electronic Hamiltonian in the frontier molecular orbital basis. The electronic interaction parameters can be computed from first principles simulations, but here they are model parameters. In arriving at the model Hamiltonian for the electronic degrees of freedom, we drop all integrals in the Hamiltonian that are three-center and higher. Physically, we suppose that the states are localized enough that three or more *different* orbitals have negligible overlap in space. This is a standard assumption that leads, for example, to the PPP Hamiltonian when atomic orbitals are the assumed basis set.[38–40] Examples of terms missing from the model electronic Hamiltonian are the Davydov splitting and the direct coupling between singlets and the triplet state.[6] When these are important, Eq. (1) is probably not a good model Hamiltonian. But when the direct coupling term between singlets and doubly excited states is dominant, the theory may also be much simpler

because the system essentially becomes a two-level system, for which any number of sophisticated theories are applicable. Detailed calculations[18] show that only three classes of states are close to the energy of the singlet monomer with the total spin angular momentum projection, $\mathcal{S}_z = 0$, diagrammed in Figure 2: the singly excited singlets, charge transfer states with three electrons on one chromophore, and doubly excited states. Guided by the results for a number of organic chromophores that exhibit singlet fission, we ignore spin-orbit coupling.[6,18] In the absence of spin-orbit coupling, the total electron spin operators $\mathcal{S}^2$ and $\mathcal{S}_z$ both commute with the Hamiltonian and are conserved. As a result of the conservation law, the states must then satisfy selection rules, which in the space of singlet excited states, means that the total electron multiplicity must always remain a singlet.[6] This also implies that $\mathcal{S}_z|\Phi\rangle = 0$ for any state $|\Phi\rangle$ in the singlet manifold. The spin-adapted linear combinations (SALC) are unitary transforms of the singlet, charge transfer, and doubly excited electronic configurations that are simultaneous eigenstates of $\mathcal{S}^2$ and $\mathcal{S}_z$ with eigenvalue 0. Note that the $|TT\rangle$ is not a two-triplet state, but is a SALC that contains doubly-excited singlet character. There are only 6 SALC that we consider. They are the ground state, $|0\rangle$, the singlet state localized on the left chromophore, $|\mathrm{S}\rangle$, the singlet state localized on the right chromophore, $|\overline{\mathrm{S}}\rangle$, the charge transfer states localized on the left ($|\mathrm{CT}\rangle$) and right ($|\overline{\mathrm{CT}}\rangle$), and the doubly excited state $|\mathrm{TT}\rangle$. This choice is not unique. Indeed, one could, for example, seek linear combinations that are delocalized across each chromophore. We choose these states rather than other linear combinations because they represent well-defined charge distributions and dipole moments on the chromophoric pair. This choice will be important in Section 3 where we couple the electronic system to a polar solvent bath. Setting the energy of the ground state to zero, and using Δ to denote the HOMO-LUMO gap, the electronic Hamiltonian in the SALC basis is diagonal with energies $E_S = E_{\overline{S}} = \Delta + \mathcal{V} - U$, $E_{CT} = E_{\overline{CT}} = \Delta + 2\mathcal{V} - U - X$, and $E_{TT} = 2(\Delta + \mathcal{V} - U) - 4/3X$. Note that the energy of the $|TT\rangle$ state is higher than the energy of the isolated triplet states by $2/3$ the exchange energy, $\frac{2X}{3}$. Had we not insisted on total spin angular momentum conservation, we would predict a lower threshold for singlet fission.

The nonzero off-diagonal matrix elements of W_{el} in the SALC basis are

$$\begin{aligned}
\langle S|W_{el}|CT\rangle &= -J_{h_R h_L} \ , \ \langle \overline{S}|W_{el}|CT\rangle = J_{l_R l_L} \ , \\
\langle S|W_{el}|\overline{CT}\rangle &= J_{l_L l_R} \ , \ \langle \overline{S}|W_{el}|\overline{CT}\rangle = -J_{h_L h_R} \ , \\
\langle CT|W_{el}|TT\rangle &= -\sqrt{\frac{2}{3}} J_{h_L l_R} \ , \ \langle \overline{CT}|W_{el}|TT\rangle = \sqrt{\frac{2}{3}} J_{h_R l_L} \ ,
\end{aligned}$$

with the remaining terms following from the Hermitian conjugate of W_{el}. The SALC, $|0\rangle$, $|S\rangle$, $|\overline{S}\rangle$, $|CT\rangle$, $|\overline{CT}\rangle$, and $|TT\rangle$ are the diabatic states of the problem (Figure 3). When all resonance integrals J_{jk} are small and the initial excitation is localized, they are the physically relevant states of the system. This is the limit in which we present the current work. Because we have neglected three-center and higher integrals, singlets do not couple to $|TT\rangle$ states directly, but rather pass through intermediate charge transfer states via electron or hole transfer in our model.[6] For example, electron transfer couples $|S\rangle$ to $|\overline{CT}\rangle$ and hole transfer couples $|S\rangle$ to $|CT\rangle$.

2.2 Hamiltonian of the dissipative system

Having specified the electronic states that couple to one another and satisfy spin selection rules, we now derive the equations of motion of the populations of the diabatic states. Experience from small polaron transport,[41] electron and energy transfer,[42–47] and spectroscopy shows that one can model the effects of the environment with the Hamiltonian,

$$H = \sum_k |k\rangle H_k \langle k| + \epsilon \sum_{k,l\neq k} |k\rangle J \langle l|. \tag{3}$$

Eq. (3) is a generic linear response Hamiltonian. The sum is over diabatic states, $|k\rangle$, J is a constant in the Condon approximation and ϵ is a parameter whose numerical value is 1, but that will order a perturbation expansion for weak coupling. Though evidently nonessential, for simplicity we assume that all couplings between diabatic states are equal, which sets all off-diagonal matrix elements of $W_{el} = J$. Assuming that the environment responds linearly when the system enters dia-

batic state $|k\rangle$, H_k can be modeled as a set of quantum-mechanical displaced harmonic oscillators,

$$H_k = E_k + \frac{1}{2}\sum_\nu \omega_\nu \left(p_\nu^2 + (q_\nu + \chi_\nu^k)^2\right). \quad (4)$$

E_k is the bare energy of diabatic state $|k\rangle$ (e.g. E_S, E_{CT}, E_{TT}, etc.). The equilibrium position of bath mode ν occurs at -χ_ν^k when the electronic system is in state $|k\rangle$. Setting $E_0 = \chi_\nu^0 = 0$ uses the ground state as a reference, so that all energy levels and fluctuations are now with respect to the ground state, $|0\rangle$. The sum is over all bath modes ν, each with frequency ω_ν, that represent the polarization fluctuations of the solvent. p_ν and q_ν are mass-weighted bath momenta and coordinates of the bath, respectively. The spectra of coupling constants between system and bath, or spectral densities,

$$\mathcal{J}_k(\omega) = \frac{\pi}{2}\sum_\nu (\omega_\nu \chi_\nu^k)^2 \, \delta(\omega - \omega_\nu),$$

completely specifies the behavior of the system. While in this work, we specialize the environment to include only solvent polarization fluctuations, it is straightforward to include molecular vibrations and phonons[45] in Eq. (4).

2.3 Equation of motion for the populations of the diabatic states

In Hilbert space, the density matrix obeys the Heisenberg equation of motion, where the Hamiltonian acts on both the right and left of the density matrix. It is convenient to work in Liouville space where one orders the density matrix elements into a vector, $\rho \rightarrow |\rho\rangle\rangle$. The equation of motion can now be written in the form, $\frac{d|\rho\rangle\rangle}{dt} = -i\mathscr{L}|\rho\rangle\rangle$, and the Liouvillian $\mathscr{L}$ acts only on the left side of the density matrix. In Liouville space inner products are defined as $\langle\langle A|B\rangle\rangle = Tr_S Tr_B\left(A^\dagger B\right)$. Tr_S is a trace over the diabatic states and Tr_B is a trace over the bath states. Choosing $H_0 = \sum_k |k\rangle H_k \langle k|$, $\hbar = 1$, and $V = \sum_{k,l\neq k} |k\rangle J \langle l|$, the full density matrix, $|\rho(t)\rangle\rangle$ obeys the quantum Liouville equation in the interaction picture,

$$\frac{d}{dt}|\hat{\rho}(t)\rangle\rangle \quad = \quad -i\epsilon\hat{\mathscr{L}}_V(t)|\hat{\rho}(t)\rangle\rangle,$$

where $\hat{\mathscr{L}}_V(t) = e^{i\mathscr{L}_0 t}\mathscr{L}_V e^{-i\mathscr{L}_0 t}$ and $|\hat{\rho}(t)\rangle\rangle = e^{-i\mathscr{L}_0 t}|\rho(t)\rangle\rangle$. One can go between the two spaces by using dual relationships between Hilbert and Liouville space in the interaction picture, such as $\hat{\mathscr{L}}_V(t)A \leftrightarrow [\hat{V}(t), A]$, $\hat{\mathscr{L}}_0 A \leftrightarrow [H_0, A]$.

The electronic population is the reduced density matrix element at time t. For state $|k\rangle$ it is $\sigma_k(t) = \langle\langle k|\rho(t)\rangle\rangle = Tr_B[\langle k|\rho(t)|k\rangle]$. Motivated by the work of Reichman and Golosov, we isolate the populations of the diabatic states using the projection operator $P = \sum_k |k\rho_k\rangle\rangle\langle\langle k|$ where ρ_k is an arbitrary, normalized, nuclear density matrix.[48,49] With the aid of the projection operator, one arrives at the formally exact (time-local) equation of motion for the populations. The equation of motion takes the form of a nonMarkovian quantum master equation,[50]

$$\frac{d}{dt}\hat{\sigma}_j(t) = -\sum_k R_{j,k}(t)\hat{\sigma}_k(t) + I_j(t). \tag{5}$$

$R_{j,k}(t)$ is an element of the relaxation matrix and $I_j(t)$ is the quantum inhomogeneous term that depends on the initial value of the density matrix in the complementary space, $(1-P)|\hat{\rho}(0)\rangle\rangle$. One often chooses projection operators so that this term is zero or it decays quickly.[51] The derivation of Eq. (5), including the forms of the relaxation operator and inhomogeneous term, are in the Appendix. Because Eq. (5) is exact, it is a convenient starting point for analysis of the electronic population dynamics. Methods for analyzing it include explicit quantum simulation via path integral and semiclassical methods,[52–54] perturbation expansions,[50,55] and asymptotic approximations.[48,49]

We expand the relaxation operator to second order in perturbation theory with respect to ϵ to find the approximate quantum master equation in the weak-coupling limit. Furthermore, we assume that the initial state is a product state so that $(1-P)|\hat{\rho}(0)\rangle\rangle = 0$ and the inhomogeneous term disappears entirely. This assumption simplifies analysis considerably, but will be re-assessed when more details about the initial conditions from experiments become available. In singlet fission, systems are necessarily multilevel, and electronic states in these systems can undergo rapid internal conversion. The initial conditions are likely to be subtle and highly system-dependent.

Expanding Eq. (5) to second order in ϵ, inserting complete sets of diabatic states, and coming out of the interaction picture yields tractable expressions for the populations,[50,56]

$$\frac{d}{dt}\sigma_j(t) = \sum_k \left[W_{k\to j}(t)\sigma_k(t) - W_{j\to k}(t)\sigma_j(t)\right] + \mathscr{O}(\epsilon^3). \tag{6}$$

$W_{j\to k}(t)$ is a time-dependent rate,

$$W_{j\to k}(t) = 2J^2 \int_0^t d\tau \mathrm{Re}\left[Tr_B\left\{e^{-iH_k\tau}e^{iH_j\tau}\rho_j(t)\right\}\right]. \tag{7}$$

Eq. (7) is the nonMarkovian generalization of Fermi's golden rule to a multilevel dissipative system. When t is long relative to the energy equilibration time in state $|k\rangle$, one can make the ergodic hypothesis, $\rho_j(t) \approx \rho_j^{(eq)}$, where $\rho_j^{(eq)} = \exp(-\beta H_j)/Z_j$, and $Z_j = Tr_B\left[\exp(-\beta H_j)\right]$. Extending the integral to infinity is equivalent to making the Markov approximation and results in Fermi's golden rule,

$$W_{j\to k} = J^2 \int_{-\infty}^{\infty} d\tau \, \langle \exp(-iH_k\tau)\exp(iH_j\tau)\rangle_j, \tag{8}$$

where $\langle\cdot\rangle_j$ is an equilibrium ensemble average with respect to state $|j\rangle$, $\langle A\rangle_j = Tr_B(A\rho_j^{(eq)})$. The nonMarkovian effects appear as transients, manifest at early times, but converge to the (time-independent) golden rule rates at long times. An example illustrating this convergence appears in Section 3. The prefactor J^2 controls the distance dependence of the rates. Because it is a resonance integral, rates should have an approximately exponential dependence on the distance between the chromophores, $W_{j\to k}(R) \sim \exp(-R/R_0)$.

2.4 Rate Theories

Assuming that each diabatic state is statistically independent[55] implies that the coupling matrix elements in Eq. (4) obey $\chi_\nu^k \chi_\mu^l = 0$ for $k \neq l$. After performing a cumulant expansion of Eq. (8), taking the trace over the bath, and using Parseval's theorem, Eq. (8) becomes the multilevel generalization

of Förster/Dexter theory applied to singlet fission,

$$W_{j\to k} = \frac{J^2}{2\pi}\int_{-\infty}^{\infty} d\omega\, A_k(\omega) I_j(\omega).$$

$A_k(\omega)$ and $I_j(\omega)$ are envelope functions related to the strength of solvent-induced fluctuations about diabatic states $|k\rangle$ and $|j\rangle$. If both states are bright, the envelope functions can be cast in terms of the absorption spectrum of state $|k\rangle$ and emission spectrum of state $|j\rangle$. The envelope functions can be written as

$$I_j(\omega) = \int_{-\infty}^{\infty} dt \exp(i\omega t)\exp\left[-i\left(E_j-\lambda_j\right)t - g_j^*(t)\right], \quad (9)$$

$$A_k(\omega) = \int_{-\infty}^{\infty} dt \exp(i\omega t)\exp\left[-i\left(E_k+\lambda_k\right)t - g_k(t)\right]. \quad (10)$$

$\lambda_j = \frac{1}{2}\sum_\nu \omega_\nu (\chi_\nu^j)^2$ is the reversible work done by the solvent to equilibrate state $|j\rangle$ from the ground state and $g_j(t)$ is a lineshape function for the energy level fluctuations in state $|j\rangle$. It can be related to the spectral density, $\mathcal{J}_j(\omega)$,

$$g_j(t) = \frac{1}{\pi}\int_0^{\infty} d\omega\, \frac{\mathcal{J}_j(\omega)}{\omega^2}\left[\coth(\beta\omega/2)(1-\cos(\omega t)) - i(\omega t - \sin(\omega t))\right]. \quad (11)$$

Dipole selection rules forbid emission or absorption to any state other than $|S\rangle$ and $|\overline{S}\rangle$, so envelope functions and associated spectral densities cannot be inferred from linear emission and absorption spectra, as they can be in Förster theory. They must be fit from experimental data, computed from molecular dynamics trajectories, or calculated with a given model for the spectral densities. In this manuscript we use model spectral densities.

3 Results and discussion

Golden rule rates depend on the spectral densities associated with their energy level fluctuations with respect to the ground state for each level. For simplicity, we assume that fluctuations in all levels are identical. For a model spectral density, we take

$$\mathcal{J}(\omega) = 2\gamma \frac{\omega\Gamma}{\omega^2 + \Gamma^2}, \tag{12}$$

which is a model spectral density applied broadly to electronic spectroscopy in polar solvents. γ is an energy scale that controls the coupling strength between the electronic states and the bath. In the high temperature limit the time correlation function for energy level fluctuations decays exponentially with a time constant of $1/\Gamma$.[57] When the timescale of energy level fluctuations is slow with respect to $1/\gamma$, each chromophore is in a static environment and the lineshape function is quadratic in time,

$$g^{\text{Slow}}(t) = k_B T \gamma t^2. \tag{13}$$

The golden rule rate from $|j\rangle$ to $|k\rangle$ is the overlap of two Gaussians, evaluated by integrating Eq. (9) using the lineshape functions in Eq. (13),

$$W_{j\to k}^{\text{Slow}} = J^2 \sqrt{\frac{\pi}{2k_B T\gamma}} \exp\left[-\frac{\left(E_k - E_j + 2\gamma\right)^2}{8k_B T\gamma}\right]. \tag{14}$$

If one identifies the solvent reorganization energy with 2γ, Eq. (14) has precisely the same form as the nonadiabatic Marcus electron transfer rate. The static limit implies inhomogeneously broadened fluctuation spectra. In the inhomogeneous limit, the envelope functions are probability distributions of a state having a given energy in the ensemble.[50] What Eq. (14) says is that only a subset of chromophores in the ensemble have the same energy in state $|k\rangle$ and $|j\rangle$, and only they can conserve energy. Because Eq. (14) is essentially a weak-coupling high temperature approximation to the rate, it is not surprising that the result is reminiscent of the Marcus theory. The role of fluctuations is evident from Eq. (14). The rate is not maximal when the bare energies E_k and

E_j are equivalent, but instead when their energy difference matches the strength of environmental fluctuations, 2γ.

Outside the slow modulation and high temperature limits, we evaluate the lineshape functions $g_j(t)$ and $g_k(t)$ by expressing the hyperbolic cotangent function in Eq. (11) as a sum over Matsubara frequencies and performing contour integrals.[58–60] Figure 4 shows the results as a function of the coupling strength, γ for off-resonant bare energies, $E_k - E_j$ = -0.1 eV at T = 300 K, and $1/\Gamma$ = 100 fs. When the energies are off-resonant, fluctuations increase the rate of transfer from $|j\rangle$ to $|k\rangle$, up to a point. Above a critical threshold, the rate decreases with increasing γ. If the coupling strength to fluctuations far exceeds $|J|$, fluctuations stabilize the diabatic states too much and thermal activation is increasingly difficult. The system becomes self-trapped.[60] This behavior is qualitatively similar to that predicted by Eq. (14) in the high-temperature static limit.

Figure 5 shows the results for the time-dependent rate of going from state $|j\rangle$ to state $|k\rangle$ as a function of time for physically reasonable values of the model parameters: $1/\Gamma$ = 100 fs, T = 300 K, γ = 0.1 eV and $E_k - E_j$ = -0.05 eV. We assume that the system has entered electronic $|j\rangle$ on a timescale much faster than the solvent or nuclei can equilibrate to that state. This can happen, for example, in a rapid interconversion process from an excited state that was prepared with an ultrafast laser pulse. The time-dependent nuclear density matrix in Eq. (7) is then $\exp(-iH_j t)\rho_g \exp(iH_j t)$, where ρ_g is the nuclear density operator for the ground state. We have evaluated this rate by making a polaron transformation, cumulant expansion and trace over the bath, and a stationary phase approximation to the integral over τ in Eq. (7) using the spectral density in Eq. (12). It is convenient to use the approximation, $\cot(x) \approx 1 + \exp(-x)/x$, which is good in the temperature range in which we study. Details of this procedure can be found in Refs. [51,55]. In the parameter range studied, the approximation to the time-dependent rate,

$$W_{j\to k}(t) \approx J^2 \sqrt{\frac{2\pi}{D(\beta)}} \exp\left[-\frac{(E_k - E_j - 2\gamma + 2C(t))^2}{2D(\beta)}\right], \tag{15}$$

where $C(t) = \gamma\exp(-\Gamma t)$ is the time-dependent reorganization energy, $\beta = 1/(k_B T)$, and $D(\beta)$ =

$\frac{2}{\pi}\int_0^\infty d\omega \mathcal{J}(\omega)(1+\frac{2}{\beta\omega}\exp(-\beta\omega/2))$, is rather accurate. This approximation makes the role of non-Markovian effects physically transparent, and accompanies the stationary-phase result in Figure 5. While the specific values for the model parameters studied here are not yet known for singlet fission experiments, the parameters used in Figure 5 are realistic for solvation dynamics in polar solvents.[37] The fact that the time-dependent rate only converges to the golden rule rate for t greater than about 600 femtoseconds should give one pause. Because singlet fission has been reported to occur on sub-picosecond timescales, these results indicate that electronic dynamics in singlet fission may fall outside the scope of a rate theory based on the golden rule even in the weak-coupling limit, and that a proper description in systems that interconvert on sub-picosecond timescales should include real-time quantum dynamics.

Finally, we comment on the multistate character of the theory, and model the polarization fluctuations from microscopic considerations. Figure 6 is a coarse-grained view, from the solvent's perspective, of the diabatic states in the problem. The singlet states experience a solvochromatic shift relative to the ground state, provided that the electron distribution is different in the excited state than in the ground state. This shift is a solvent response to an *intramolecular* dipole moment that occurs when the chromophore enters the electronically excited state. An *intermolecular*, or more precisely interchromophoric, dipole moment relative to the ground state characterizes the charge transfer states. These states experience a reorganization energy from the solvent in the Marcus sense. If only singlets and charge transfer states were involved, one could simply apply the theories of photoinduced electron transfer. But the charge transfer states are intermediates between the singlets and the $|TT\rangle$ state. Relative to the charge transfer states, the solvent must relax an intermolecular dipole moment *and* accommodate an additional electronic excitation in the $|TT\rangle$ state. To model these phenomena, we assume that the system begins in state $|S\rangle$, and the solvent has equilibrated to that electronic charge distribution. To make progress in this direction, we rewrite H_0 in the canonical "system plus bath" form, $H_0 = H_S + H_{SB} + H_B$. H_0 is still diagonal

in the diabatic basis but we propose that H_{SB} should be

$$H_{SB} = (n_R - n_L)\sum_\nu \omega_\nu \Lambda_\nu q_\nu + (n^* - 1)\sum_\nu \omega_\nu \lambda_\nu q_\nu. \tag{16}$$

$n_R - n_L$ is the total number of electrons on the right chromophore minus the number of electrons on the left chromophore, while n^* is the number of electrons in the LUMO orbitals. The form of Eq. (16) ensures that the bath responds *linearly* to the change in the dipole moments relative to state $|S\rangle$. For simplicity, we assume that intermolecular and intramolecular polarization fluctuations are uncorrelated by imposing $\lambda_\nu \Lambda_\nu = 0$. In the high-temperature limit, the transfer rates between $|S\rangle$ and $|\overline{CT}\rangle$, and from $|\overline{CT}\rangle$ to $|TT\rangle$ assume the form of a Marcus rate,

$$W_{S\to\overline{CT}} = J^2\sqrt{\frac{\pi\beta}{\Lambda}}e^{-\frac{\beta}{4\Lambda}\left(E_{\overline{CT}} - E_S + \Lambda\right)^2}, \tag{17}$$

$$W_{CT\to TT} = J^2\sqrt{\frac{\pi\beta}{\lambda+\Lambda}}e^{-\frac{\beta}{4(\lambda+\Lambda)}\left(E_{TT} - E_{\overline{CT}} + \lambda + \Lambda\right)^2}.$$

$\Lambda = \frac{1}{2}\sum_\nu \omega_\nu \Lambda_\nu^2$ is the reorganization energy associated with interchromophoric electron transfer and $\lambda = \frac{1}{2}\sum_\nu \omega_\nu \lambda_\nu^2$ is the reorganization energy for intramolecular charge redistribution in the excited state. It is related to the Stokes shift. Because the solvent must do more work to accomodate the charge distribution in the $|TT\rangle$ state, the rates in Eq. (17) indicate that the inverted regime occurs at higher energies for the $W_{\overline{CT}\to TT}$ than for $W_{S\to\overline{CT}}$. Figure 7 (B) is a plot for the forward transfer rates, $W_{S\to\overline{CT}}$ and $W_{\overline{CT}\to TT}$ compared to the back transfer rates $W_{\overline{CT}\to S}$ and $W_{TT\to\overline{CT}}$ for the energy level stagger between $|S\rangle$ and $|TT\rangle$ fixed as a function of the energy for the charge transfer intermediate $|\overline{CT}\rangle$. The specific parameters appear in the figure caption. Figure 7 indicates a region where $E_S > E_{\overline{CT}} > E_{TT}$ (between the dotted blue lines), where the forward rates exceed the back transfer rates. The weak-coupling high-temperature result predicts the non-Ahrennius behavior characteristic of Marcus electron transfer. While this is not particularly surprising, Figure 4 illustrates the interplay between energy level spacings and solvent fluctuations as a design principle for maximizing singlet fission yields. Even if the bare energy levels are not resonant,

environmental fluctuations make the rates nonzero.

We have presented a model for singlet fission in the presence of solvation-induced energy level fluctuations and analyzed it using model parameters for electronic energy levels, electronic coupling, and spectral densities in the weak-electronic coupling limit. The model electronic Hamiltonian employed allowed us to identify selection rules and approximate energies of electronic configurations. Enforcing total angular momentum spin conservation predicts that degeneracy between the singly excited singlet states and the doubly excited $|TT\rangle$ state should occur at a slightly higher energy than that of the isolated triplets. This is because one needs to include the doubly excited spin singlets to satisfy total spin angular momentum conservation. This is vaguely reminiscent of theories of MEG in nanocrystals and carbon nanotubes, where selection rules delay the onset of MEG, although the matrix elements evaluated there are different. It would be interesting to check this prediction against more detailed electronic structure calculations. Though we did not follow this route for reasons of consistency, if the $|S\rangle$ and $|TT\rangle$ states are directly coupled, as some have suggested for molecules like pentacene,[6] it is simple to redefine the diabatic states and extend the results of Section 2.3 to describe this case. Using a reasonable initial density matrix and model parameters for energy level splittings and solvent reorganization energies, we find that the non-Markovian aspects of electron dynamics in singlet fission may be significant on sub-picosecond timescales. One should apply the golden rule with caution when dynamics occur on timescales of less than a picosecond, even in the limit of weak coupling. Finally, while we have assumed the weak electronic coupling limit in this work, this assumption is probably marginal in some cases. Recent work has found coupling matrix elements that range between 0.02 to 0.1 eV. If the reorganization energy is not larger than this energy scale, the weak-electronic coupling limit is not valid. If the electronic coupling matrix elements are larger than the reorganization energies, then one should analyze the density matrix dynamics with Redfield theory or one of its variants.[57,61] If the reorganization energies and electronic coupling matrix elements are of the same size, which may be the case in some systems, perturbative approaches are not trustworthy.[62] While there is still much theoretical and experimental work that needs to be done to understand what controls

electronic energy levels and coupling, we hope the current work will help empower the sophisticated tools of condensed phase chemical physics: nonlinear spectroscopy, molecular dynamics simulations, and quantum dynamical theory, to build a comprehensive picture of singlet fission.

4 Acknowledgements

The authors thank Josef Michl for interesting discussions. J.D.E thanks the University of Colorado for generous startup funds.

5 Appendix

We can solve the Liouville equation in the complementary space by defining $Q = 1 - P$ and solving for $Q|\hat{\rho}(t)\rangle\rangle$, which is given by

$$Q|\hat{\rho}(t)\rangle\rangle = \mathscr{G}_Q^+(t,0)Q|\hat{\rho}(0)\rangle\rangle - i\epsilon \int_0^t d\tau \mathscr{G}_Q^+(t,\tau)Q\hat{\mathscr{L}}_V(\tau)P|\hat{\rho}(\tau)\rangle\rangle$$

using the time evolution operators

$$g_-(t,\tau) = \hat{T}_- exp\Big[i\epsilon \int_\tau^t ds\hat{\mathscr{L}}_V(s)\Big]$$
$$\mathscr{G}_Q^+(t,\tau) = \hat{T}_+ exp\Big[-i\epsilon Q \int_\tau^t ds\hat{\mathscr{L}}_V(s)\Big]$$

where $\hat{T}_+$ and $\hat{T}_-$ denote forward and backward time evolution, respectively. This solution can be recast as

$$Q|\hat{\rho}(t)\rangle\rangle = [1 - \Sigma(t)]^{-1}[\mathscr{G}_Q^+(t,0)Q|\hat{\rho}(0)\rangle\rangle + \Sigma(t)P|\hat{\rho}(t)\rangle\rangle] \quad (18)$$

where the $\Sigma(t)$ operator is given by[50]

$$\Sigma(t) = -i\epsilon \int_0^t d\tau \mathscr{G}_Q^+(t,\tau)Q\hat{\mathscr{L}}_V(\tau)Pg_-(t,\tau).$$

When Eq. (18) is introduced into our reduced space we get the exact solution

$$\frac{d}{dt}P|\hat{\rho}(t)\rangle\rangle = -i\epsilon P\hat{\mathscr{L}}_V(t)P|\hat{\rho}(t)\rangle\rangle - i\epsilon P\hat{\mathscr{L}}_V(t)[1-\Sigma(t)]^{-1}\Big[\mathscr{G}_Q^+(t,0)Q|\hat{\rho}(0)\rangle\rangle + \Sigma(t)P|\hat{\rho}(t)\rangle\rangle\Big]. \quad (19)$$

Operating from the left with $\langle\langle j|$ on Eq. (19) we get

$$\frac{d}{dt}\hat{\sigma}_j(t) = -\sum_k R_{j,k}(t)\hat{\sigma}_k(t) + I_j(t) \quad (20)$$

having defined

$$R_{j,k}(t) = i\epsilon\langle\langle j|\hat{\mathscr{L}}_V(t)[1-\Sigma(t)]^{-1}|k\rho_k\rangle\rangle$$
$$I_j(t) = -i\epsilon\langle\langle j|\hat{\mathscr{L}}_V(t)[1-\Sigma(t)]^{-1}\mathscr{G}_Q^+(t,0)Q|\hat{\rho}(0)\rangle\rangle.$$

Using the simplification that $P\hat{\mathscr{L}}_V P = 0$ we expand Eq. (20) to $\mathscr{O}(\epsilon^2)$ which leads to Eq. (6) and Eq. (7).

References

(1) Shockley, W.; Queisser, H. J. *J. Appl. Phys.* **1961**, *32*, 510–519.

(2) Hanna, M. C.; Nozik, A. J. *J. Appl. Phys.* **2006**, *100*, 074510(1–8).

(3) Shabaev, A.; Efros, A. L.; Nozik, A. J. *Nano Lett.* **2006**, *6*, 2856–2863.

(4) Nozik, A. J. *Nano. Lett.* **2010**, *10*, 2735–2741.

(5) Franceschetti, A.; An, J. M.; Zunger, A. *Nano Lett.* **2006**, *6*, 2191–2195.

(6) Smith, M. B.; Michl, J. *Chem. Rev.* **2010**, *110*, 6891–6936.

(7) Antognazza, M. R.; Luer, L.; Polli, D.; Christensen, R. L.; Schrock, R. R.; Lanzani, G.; Cerullo, G. *Chem. Phys.* **2010**, *373*, 115–121.

(8) Kuhlman, T. S.; Kongsted, J.; Mikkelsen, K. V.; Møller, K. B.; Sølling, T. I. *J. Am. Chem. Soc.* **2010**, *132*, 3431–3439.

(9) Wilson, M. W. B.; Rao, A.; Clark, J.; Kumar, R. S. S.; Brida, D.; Cerullo, G.; Friend, R. H. *J. Am. Chem. Soc.* **2011**, *133*, 11830–11833.

(10) Chan, W.-L.; Ligges, M.; Jailaubekov, A.; Kaake, L.; Miaja-Avila, L.; Zhu, X.-Y. *Science* **2011**, *334*, 1541–1545.

(11) Yamagata, H.; Norton, J.; Hontz, E.; Olivier, Y.; Beljonne, D.; Brédas, J. L.; Silbey, R. J. *J. Chem. Phys.* **2011**, *134*, 204703(1–11).

(12) Johnson, R. C.; Merrifield, R. E. *Phys. Rev. B* **1970**, *1*, 896–902.

(13) Merrifield, R. E. *J. Chem. Phys.* **1968**, *48*, 4318–4319.

(14) Jadhav, P. J.; Mohanty, A.; Sussman, J.; Lee, J.; Baldo, M. A. *Nano Lett.* **2011**, *11*, 1495–1498.

(15) Lee, J.; Jadhav, P.; Baldo, M. A. *Appl. Phys. Lett.* **2009**, *95*, 033301(1–3).

(16) Zimmerman, P. M.; Zang, Z.; Musgrave, C. B. *Nat. Chem.* **2010**, *2*, 648–652.

(17) Zimmerman, P. M.; Bell, F.; Casanova, D.; Head-Gordon, M. *J. Am. Chem. Soc.* **2011**, *133*, 19944–19952.

(18) Greyson, E. C.; Vura-Weis, J.; Michl, J.; Ratner, M. A. *J. Phys. Chem. B* **2010**, *114*, 14168–14177.

(19) Tornow, S.; Bulla, R.; Anders, F. B.; Nitzan, A. *Phys. Rev. B* **2008**, *78*, 035434(1–14).

(20) Greyson, E. C.; Stepp, B. R.; Chen, X.; Schwerin, A. F.; Paci, I.; Smith, M. B.; Akdag, A.; Johnson, J. C.; Nozik, A. J.; Michl, J.; et al., *J. Phys. Chem. B* **2010**, *114*, 14223–14232.

(21) Todd, M. D.; Nitzan, A.; Ratner, M. A. *J. Phys. Chem.* **1993**, *97*, 29–33.

(22) Grätzel, M.; Hagfeldt, A. *Acc. Chem. Res.* **2000**, *33*, 269–277.

(23) Brédas, J.; Beljonne, D.; Coropceanu, V.; Cornil, J. *Chem. Rev.* **2004**, *104*, 4971–5004.

(24) Gruhn, N. E.; da Silva Filho, D. A.; Bill, T. G.; Malagoli, M.; Coropceanu, V.; Kahn, A.; Brédas, J. *J. Am. Chem. Soc.* **2002**, *124*, 7918–7919.

(25) McMahon, D. P.; Troisi, A. *J. Phys. Chem. Lett.* **2010**, *1*, 941–946.

(26) Schatz, G. C.; Ratner, M. A. *Quantum Mechanics in Chemistry*; Dover, New York, 2002.

(27) Pope, M.; Swenberg, C. E. *Electronic Processes in Organic Crystals and Polymers*; Oxford University Press, Oxford, U.K., 1999; pp 134–191.

(28) Thorsmølle, V. K.; Averitt, R. D.; Demsar, J.; Smith, D. L.; Tretiak, S.; Martin, R. L.; Chi, X.; Crone, B. K.; Ramirez, A. P.; Taylor, A. J. *Phys. B (Amsterdam, Neth.)* **2009**, *404*, 3127–3130.

(29) Thorsmlle, V. K.; Averitt, R. D.; Demsar, J.; Smith, D. L.; Tretiak, S.; Martin, R. L.; Chi, X.; Crone, B. K.; Ramirez, A. P.; Taylor, A. J. *Phys. Rev. Lett.* **2009**, *102*, 017401(1–4).

(30) Tiago, M. L.; Northrup, J. E.; Louie, S. G. *Phys. Rev. B* **2003**, *67*, 115212(1–6).

(31) Barbara, P. F.; Meyer, T. J.; Ratner, M. A. *J. Phys. Chem.* **1996**, *100*, 13148–13168.

(32) Förster, T. In *In Modern Quantum Chemistry, Pt. III*; Sinanoglu, O., Ed.; Academic, New York, 1965.

(33) Perdomo, A.; Vogt, L.; Najmaje, A.; Aspuru-Guzik, A. *Appl. Phys. Lett.* **2010**, *96*, 093114(1–3).

(34) Chandler, D.; Bader, J. S. *Chem. Phys. Lett.* **1989**, *157*, 501–504.

(35) Bader, J. S.; Kuharski, R. A.; Chandler, D. *J. Chem. Phys.* **1990**, *93*, 230–236.

(36) Rosenthal, S. J.; Jimenez, R.; Fleming, G. R.; Kumar, P. V.; Maroncelli, M. *J. Mol. Liq.* **1994**, *60*, 25–26.

(37) Eaves, J. D.; Tokmakoff, A.; Geissler, P. L. *J. Phys. Chem. A* **2005**, *109*, 9424–9436.

(38) Koutecký, J. *J. Chem. Phys.* **1967**, *47*, 1501–1511.

(39) Pariser, R.; Parr, R. G. *J. Chem. Phys.* **1953**, *21*, 466–471.

(40) Pople, J. A. *Trans. Faraday Soc.* **1953**, *49*, 1375–1385.

(41) Mahan, G. D. *Many Particle Physics 3rd ed.*; Kluwer Academic/Plenum Publishers, New York, 2000.

(42) Jortner, J. *J. Chem. Phys.* **1976**, *64*, 4860–4867.

(43) Bixon, M.; Jortner, J. *Chem. Phys.* **1993**, *176*, 467–481.

(44) Bixon, M.; Jortner, J. *Faraday Discuss. Chem. Soc.* **1982**, *74*, 17–29.

(45) Jortner, J.; Ulstrup, J. *J. Chem. Phys.* **1975**, *63*, 4358–4368.

(46) Marcus, R. A. *J. Chem. Phys.* **1956**, *24*, 966–978.

(47) Marcus, R. A.; Sutin, N. *Biochim. Biophys. Acta* **1985**, *811*, 265–322.

(48) Golosov, A. A.; Reichman, D. R. *J. Chem. Phys.* **2001**, *115*, 9848–9861.

(49) Sparpaglione, M.; Mukamel, S. J. *J. Chem. Phys.* **1988**, *88*, 3263–3280.

(50) Chang, T.; Skinner, J. *Phys. A (Amsterdam, Neth.)* **1993**, *193*, 483–539.

(51) Jang, S.; Cheng, Y.; Reichman, D. R.; Eaves, J. D. *J. Chem. Phys.* **2008**, *129*, 101104(1–4).

(52) Sim, E.; Makri, N. *Comput. Phys. Commun.* **1997**, *99*, 335–354.

(53) Golosov, A. A.; Friesner, R. A.; Pechukas, P. *J. Chem. Phys.* **1999**, *110*, 138–146.

(54) Evans, D. G.; Nitzan, A.; Ratner, M. A. *J. Chem. Phys.* **1998**, *108*, 6387–6393.

(55) Jang, S.; Jung, Y.; Silbey, R. J. *Chem. Phys.* **2002**, *275*, 319–332.

(56) Laird, B. B.; Budimir, J.; Skinner, J. L. *J. Chem. Phys.* **1991**, *94*, 4391–4404.

(57) Fleming, G. R.; Ishizaki, A. *J. Chem. Phys.* **2009**, *130*, 234110(1–8).

(58) Bosma, W. B.; Yan, Y. J.; Mukamel, S. *Phys. Rev. A* **1990**, *42*, 6920–6923.

(59) Tanimura, Y.; Mukamel, S. *Phys. Rev. E* **1993**, *47*, 118–136.

(60) Weiss, U. *Quantum Dissipative Systems*; World Scientific, Singapore, 1993.

(61) Fleming, G. R.; Yang, M. *Chem. Phys.* **2002**, *275*, 355–372.

(62) Ishizaki, A.; Fleming, G. R. *Proc. Natl. Acad. Sci. U. S. A.* **2009**, *106*, 17255–17260.

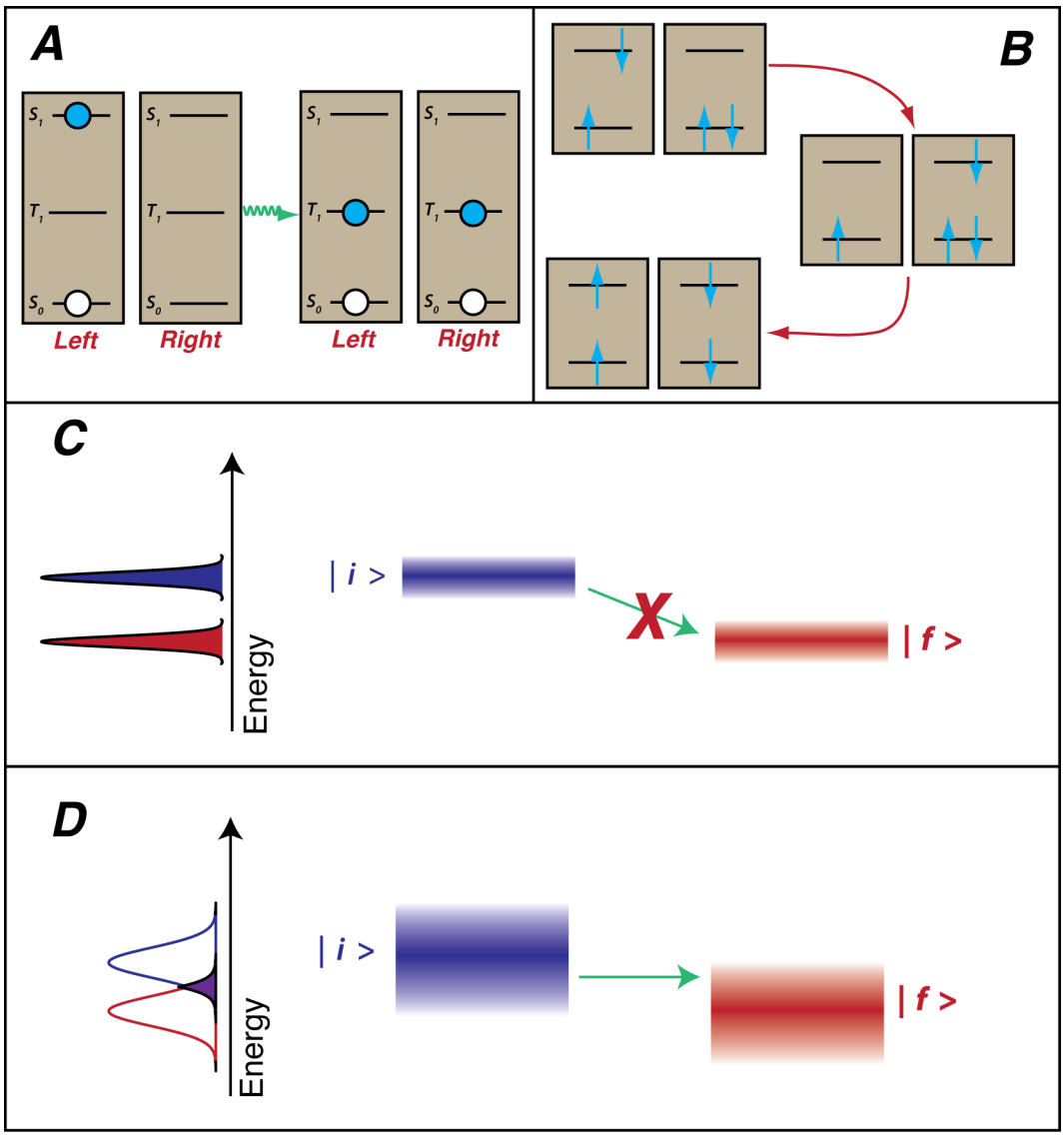

Figure 1: Conceptual diagram of singlet fission and the role of fluctuations. **(A)** Two chromophores, Left and Right, have energy levels where the triplet state is nearly half the energy of the singlet S_1 state. The electron (solid blue circle) and hole (empty circle) undergo singlet fission, which is an internal conversion process that leaves the system with two excitations, one on each chromophore. **(B)** Electronic configurations that participate in singlet fission. A singlet (top) can go through a charge transfer state (middle) and then to a doubly excited state (bottom). The states in both **A** and **B** are *schematic* because if taken literally, these states are not eigenstates of the total electron spin angular momentum. In addition to satisfying spin selection rules, interconversion must satisfy energy conservation. An initial state, $|i\rangle$, cannot transition to another state, $|f\rangle$, unless energy is conserved. For a system in relative isolation **(C)**, a large energy difference between states forbids transitions. In **(D)**, the solvent induces energy level fluctuations that broaden the relevant densities of states between $|i\rangle$ and $|f\rangle$. Provided that selection rules are satisfied, transitions can occur when two states have the same energies (purple overlap).

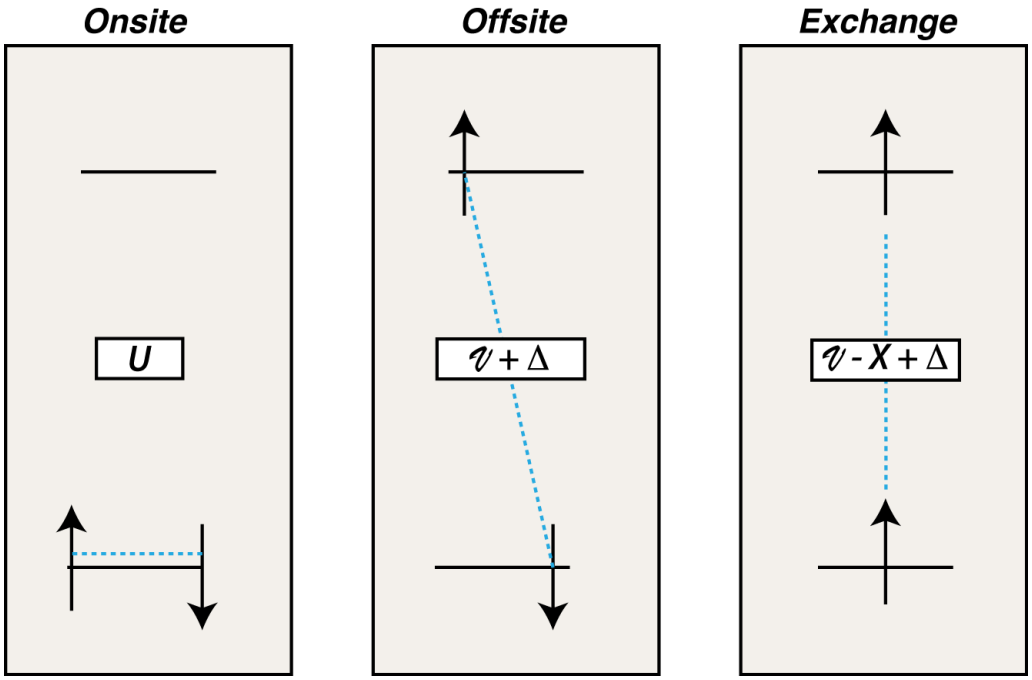

Figure 2: Energy level diagrams for electron-electron interactions in Eq. (1). Each panel represents an electronic state of a chromophore. When two electrons are in the same molecular orbital, they experience an "onsite" Coulomb repulsion U, while two electrons on the same chromophore experience an "offsite" Coulomb repulsion $\mathcal{V}$. The HOMO-LUMO gap is Δ, and the exchange energy is X. The coupling, J, allows electrons to move between chromophores in one-electron steps, or hops.

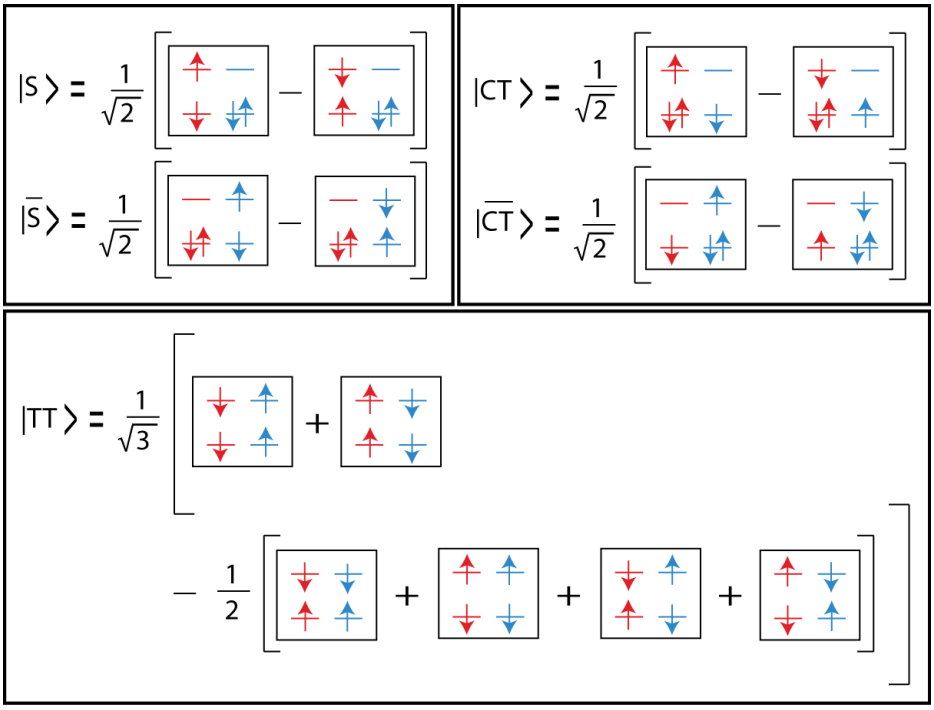

Figure 3: Spin-adapted linear combinations in the total singlet manifold that exploit spin symmetry and block-diagonalize the total Hamiltonian. Red levels belong to the left chromophore and blue levels denote the right chromophore. The levels are physically-motivated, mutually orthogonal molecular orbitals, for which the matrix elements in Eq. (1) are evaluated. Only five singly and doubly excited states in this system will be simultaneous eigenstates of the total electron spin operators $\mathcal{S}^2$ and $\mathcal{S}_z$ with eigenvalue zero. We denote the many-body electronic states in the number occupation basis as $|h_L, l_L; h_R, l_R\rangle$, where, for example, h_L is the HOMO on the left chromophore and l_R is the LUMO on the right chromophore. As an example, the singlet excited state localized on the left chromophore in the number occupation basis is $|\mathrm{S}\rangle = \frac{1}{\sqrt{2}}(|\downarrow,\uparrow;\uparrow\downarrow,0\rangle - |\uparrow,\downarrow;\uparrow\downarrow,0\rangle)$.

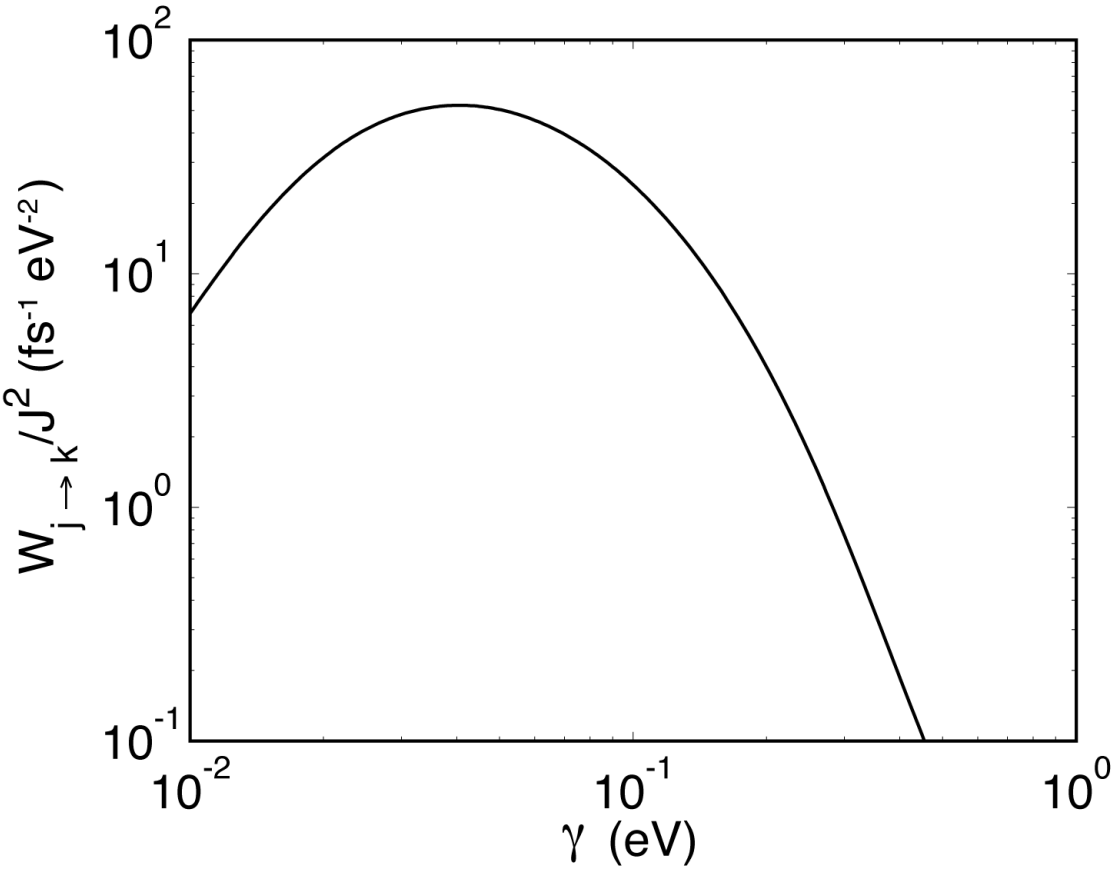

Figure 4: The golden rule rate from state $|j\rangle$ to $|k\rangle$ as a function of the system-bath coupling energy γ. $E_k - E_j$ = -0.1 eV at T = 300 K, and $1/\Gamma$ = 100 fs (See text). The energy levels are off resonance and fluctuations enhance the rate of transfer until the system enters the self-trapping regime.[60]

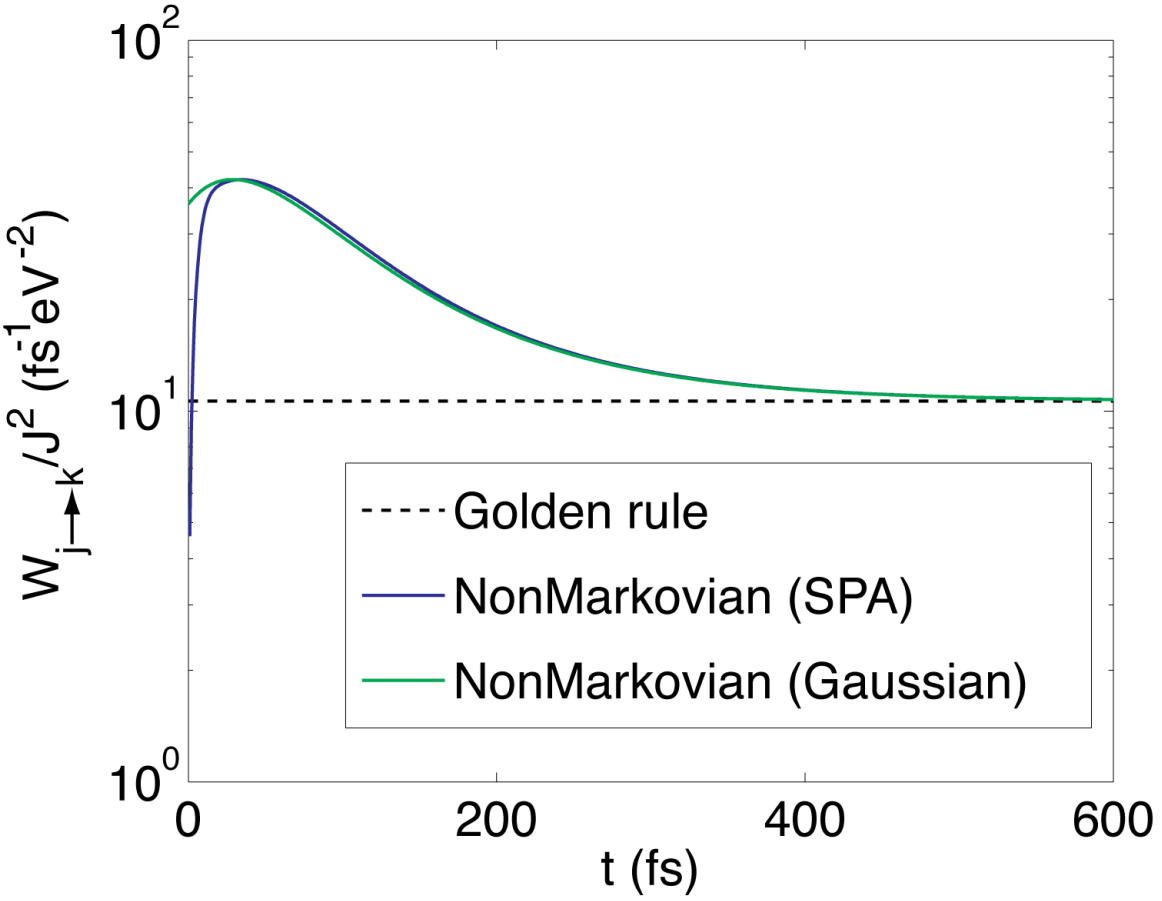

Figure 5: The nonMarkovian rate and golden rule rate from state $|j\rangle$ to $|k\rangle$ as a function of time. $E_k - E_j$ = -0.05 eV at T = 300 K, $1/\Gamma$ = 100 fs and γ = 0.1 eV (See text). The stationary phase approximation (SPA) to the nonMarkovian rate shows good agreement with the approximate form in Eq. (15). The nonMarkovian rate converges to the golden rule rate, but only for times greater than about 600 fs.

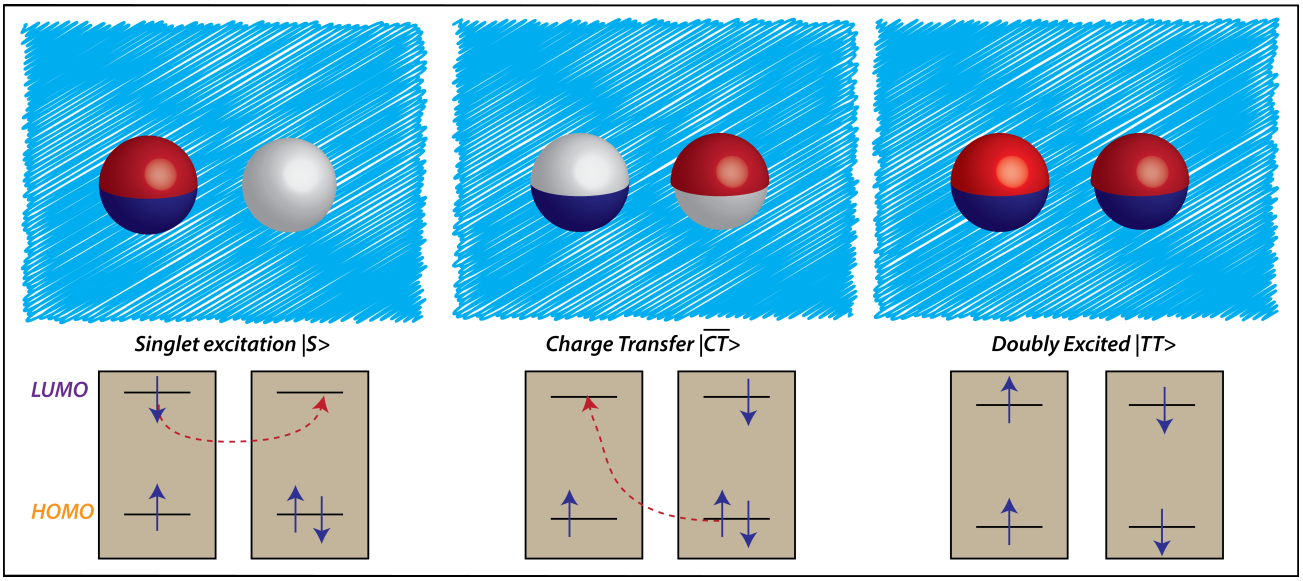

Figure 6: Schematic of the charge distribution on each chromophore in the $|S\rangle$, $|\overline{CT}\rangle$, and $|TT\rangle$ states. Blue and red colors denote charge differences relative to the ground state. The SALC states are linear combinations of states of the same polarization, only with different spin configurations. The solvent responds to the charge, not the spin. If the system starts with the solvent equilibrated in the $|S\rangle$ state, an electron transfer event brings the $|S\rangle$ state to $|\overline{CT}\rangle$, while *both* an electron transfer and an intramolecular charge redistribution must occur in the $|TT\rangle$ state when coming from the $|\overline{CT}\rangle$ state. The model system-bath Hamiltonian in Eq. (16) takes these considerations into account.

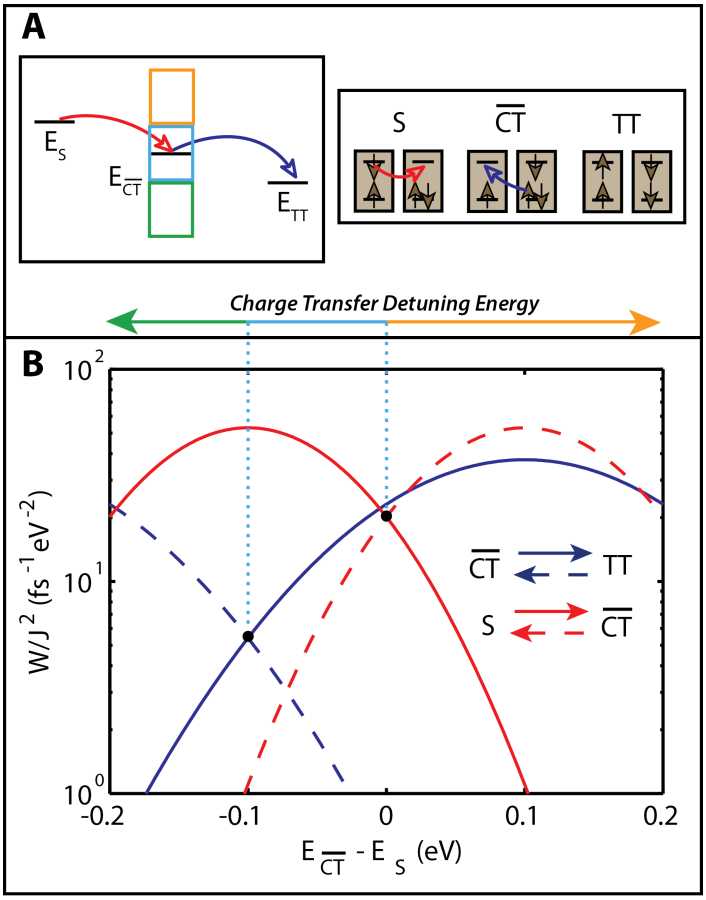

Figure 7: (**A**) The “mediated" two electron process as a function of energy level stagger for E_S and E_{TT} fixed with $E_{\overline{CT}}$ varying. The orange rectangle signifies the region where $E_{\overline{CT}} > E_S$, the green rectangle denotes the region where $E_{\overline{CT}} < E_{TT}$, and the blue region is where $E_S > E_{\overline{CT}} > E_{TT}$. Schematic configurations in the top right panel illustrate one-electron electron transfer events. (**B**) Marcus rates in the high temperature limit for $T = 300K$, $\Lambda = \lambda = 0.1$ eV, $E_{TT} = -0.1eV$. The extra reorganization energy for the $|\overline{CT}\rangle \rightarrow |TT\rangle$ increases the width of the $W_{\overline{CT}\rightarrow TT}$ rate relative to that of the $W_{S\rightarrow\overline{CT}}$ rate. Forward rates are solid lines and back transfer rates are dashed. The dotted vertical light blue lines represent the “window of opportunity" for singlet fission, where $E_S > E_{\overline{CT}} > E_{TT}$, and terminate on the black dots where forward and back transfer rates are equivalent. In the window of opportunity, all forward transfer rates are larger than the back transfer rates.

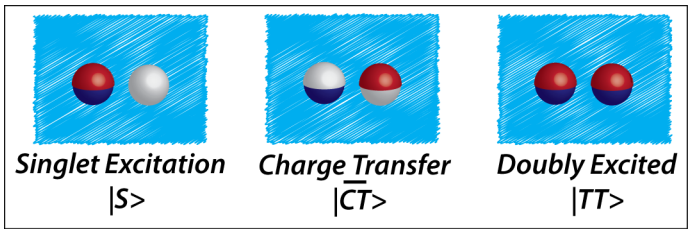
Singlet Excitation
|S>
Charge Transfer
|CT>
Doubly Excited
|TT>